Taylor & Francis
Taylor & Francis Group

RESEARCH ARTICLE

Moving beyond size and phosphatidylserine exposure: evidence for a diversity of apoptotic cell-derived extracellular vesicles *in vitro*

Ivan K. H. Poon [iD][a], Michael A. F. Parkes[a], Lanzhou Jiang[a], Georgia K. Atkin-Smith[a], Rochelle Tixeira[a], Christopher D. Gregory[b], Dilara C. Ozkocak[a], Stephanie F. Rutter[a], Sarah Caruso[a], Jascinta P. Santavanond[a], Stephanie Paone[a], Bo Shi[a], Amy L. Hodge[a], Mark D. Hulett[a], Jenny D. Y. Chow[a], Thanh Kha Phan[a] and Amy A. Baxter[a]

[a]Department of Biochemistry and Genetics, La Trobe Institute for Molecular Science, La Trobe University, Melbourne, Australia; [b]MRC Centre for inflammation Research, Queen's Medical Research Institute, University of Edinburgh, Edinburgh, UK

ABSTRACT

Apoptosis is a form of programmed cell death that occurs throughout life as part of normal development as well as pathologic processes including chronic inflammation and infection. Although the death of a cell is often considered as the only biological outcome of a cell committed to apoptosis, it is becoming increasingly clear that the dying cell can actively communicate with other cells via soluble factors as well as membrane-bound extracellular vesicles (EVs) to regulate processes including cell clearance, immunity and tissue repair. Compared to EVs generated from viable cells such as exosomes and microvesicles, apoptotic cell-derived EVs (ApoEVs) are less well defined and the basic criteria for ApoEV characterization have not been established in the field. In this study, we will examine the current understanding of ApoEVs, in particular, the ApoEV subtype called apoptotic bodies (ApoBDs). We described that a subset of ApoBDs can be larger than 5 µm and smaller than 1 µm based on flow cytometry and live time-lapse microscopy analysis, respectively. We also described that a subset of ApoBDs can expose a relatively low level of phosphatidylserine on its surface based on annexin A5 staining. Furthermore, we characterized the presence of caspase-cleaved proteins (in particular plasma membrane-associated or cytoplasmic proteins) in samples enriched in ApoBDs. Lastly, using a combination of biochemical-, live imaging- and flow cytometry-based approaches, we characterized the progressive lysis of ApoBDs. Taken together, these results extended our understanding of ApoBDs.

Introduction

Major EV subtypes including exosomes and microvesicles are recognized as key regulators of intercellular communication and could participate in processes such as inflammation, immune responses, coagulation, tumorigenesis and host–microbe interactions [1–6]. Furthermore, a number of studies have proposed the use of EV subtypes and EV-associated contents as biomarkers for pathologic conditions including cardiovascular, autoimmune and neurodegenerative diseases [1–6]. Therefore, the field has made a significant effort to better define EVs generated from viable cells, and establish extensive guidelines for studying them [7–11]. In contrast, EVs derived from apoptotic cells (denoted as ApoEVs) are generally less well defined, with most studies in the field of EVs and cell death systematically removing them from analysis rather than performing detailed characterization. It has been estimated that up to 100–150 billion cells will die via apoptosis daily in the human body to maintain homeostasis [12,13], and the frequency of apoptosis is higher in disease settings including infection [14,15], as well as medical interventions like in chemo-/radio-therapy [16,17]. Thus, ApoEVs are a major subtype of EVs from apoptotic cells that could be released under physiologically relevant settings and their properties need to be better defined.

ApoEVs is a broad term that can be used to describe EVs generated from apoptotic cells [18]. Larger ApoEVs are categorized as ApoBDs (generally considered as 1–5 µm in diameter based on light and electron microscopy studies) [3,19–22], whereas smaller ApoEVs are described as apoptotic microvesicles (ApoMVs, generally considered as 0.1–1 µm in diameter) based on their size similarities with microvesicles generated from viable cells [1,3]. Recently,

exosome-like vesicles (<150 nm) that are released during the progression of apoptosis were also characterized [23]. It is worth noting that different subtypes of ApoEVs may exhibit different functional properties. For example, ApoBDs but not ApoMVs generated from stress-activated apoptotic human endothelial cells were able to drive sterile inflammation through the trafficking of IL-1α [24]. Thus, it is important to distinguish different ApoEV subtypes. In this study, we will focus on ApoBDs and how we could better define this ApoEV subtype. It should be noted that different ApoEV subtypes may overlap in size and whether size is the best criterion to distinguish different ApoEV subtypes is debatable. Nevertheless, since there is currently no single parameter to clearly distinguish ApoBDs from other ApoEV subtypes, we will continue to use the size-based definition as described above in this study. It is worth noting that ApoBDs are also described in the literature (e.g. in primary research [25–29] and review articles [30–32]) as EVs that are "0.05–5 μm" or "<1.2 μm" in diameter, and we will not adopt this description as it does not account for different ApoEV subtypes.

Based on the size of ApoBDs, they can be easily visualized by standard light and electron microscopy [33–38], and quantified in a semi high-throughput manner by flow cytometry [39–42], image-based flow cytometry [36] and tunable resistive pulse sensing [43,44]. In addition to simply detecting vesicles that are 1–5 μm in diameter to conclude the presence of ApoBDs in a sample, hallmarks of apoptosis can also be monitored to provide further evidence that ApoBDs are indeed formed under specific experimental conditions [24,36,40,45–47]. Hallmarks of apoptosis (e.g. caspase activation, DNA fragmentation) are well defined [33,48–50], and more recently, morphological steps of apoptotic cell disassembly (the process of ApoBD formation) are beginning to be characterized in detail [36,40,45,51,52]. Since ApoBDs can only be generated during apoptosis and after distinct morphological steps of apoptotic cell disassembly have occurred, a number of studies have validated these events in addition to detecting the presence of vesicles that are between 1 and 5 μm in diameter [24,36,42,43,45,51,53,54]. Thus, for *in vitro* studies, it is important to monitor the level of apoptosis from cells that have generated ApoBDs. Likewise, monitoring the morphological steps of apoptotic cell disassembly, namely plasma membrane blebbing, thin membrane protrusion formation (e.g. apoptopodia) and the generation of distinct ApoBDs (i.e. not blebs that are still on the surface of the apoptotic cell) will provide clear evidence that ApoBDs are indeed generated from cells undergoing apoptosis. For tissue samples, ApoBDs can also be readily observed by electron microscopy along with other hallmarks of apoptosis such as nuclear condensation and organelle fragmentation [33,48,55], thus further confirming the identification of ApoBDs. Although ApoBDs can be easily visualized as they are one of the largest types of extracellular vesicles, many properties of ApoBDs are yet to be fully characterized. To better understand the nature of ApoBDs, certain properties of ApoBDs such as size, markers and membrane permeability will be examined and/or discussed in this study to help establish suitable criteria for studies of ApoBDs. It should be noted that the purpose of this study is not to propose strict rules to define ApoBDs but to highlight parameters investigators should consider when studying ApoBDs.

Materials and methods

Cell lines and tissue culture

Human LIM1215 colorectal epithelial cells were gifted from Dr Suresh Mathivanan (La Trobe University, Australia), human THP-1 monocytic and Jurkat T (clone E6-1) cells were obtained from ATCC (TIB-202 and TIB-152, respectively). PANX1$^{-/-}$ GFP$^+$ mCherry$^+$ (clonal) Jurkat T cells were generated by a CRISPR/Cas9-based approach [56]. All cell lines were cultured at 37°C in a humidified atmosphere with 5% CO_2, in RPMI 1640 medium (Life Technologies) supplemented with 5% fetal bovine serum (FBS) (Gibco), penicillin (50 U/ml) and streptomycin (50 μg/ml) (Thermo Fisher Scientific), and MycoZap (0.2% v/v) (Lonza).

Apoptosis induction

Unless stated otherwise, cells for apoptosis induction were prepared in serum-free RPMI supplemented with 1% bovine serum albumin (BSA). Apoptosis was induced via UV irradiation (150 mJ/cm^2) using a Stratalinker UV Crosslinker 1800 (Agilent Technologies) followed by incubation at 37°C under a humidified atmosphere with 5% CO_2 for indicated times. The formation of ApoBDs by cells undergoing apoptosis, including the morphological steps of apoptotic cell disassembly, following UV irradiation was characterized extensively in previous studies [36,45] and level of apoptosis and ApoBD formation validated by flow cytometry as described below. It should be noted that ApoBD-like vesicles were not detected in

1% BSA/RPMI or 5% FBS/RPMI (Supplementary Figure 1, Supplementary Video 1, 2 and 3).

Preparation of ApoBD depleted and ApoBD enriched samples

ApoBD depleted and ApoBD enriched samples were prepared via a differential centrifugation approach as described previously [57]. Briefly, THP-1 and Jurkat T cells were collected 3–4 h post apoptosis induction and pelleted by centrifugation (Allegra® X-15R Centrifuge, SX4750/SX4750A, Beckman Coulter) at 300 g for 10 min to pellet cells (viable, apoptotic, necrotic cells) and some large ApoBDs (i.e. ApoBD depleted sample). The supernatant was then collected and centrifugation at 3,000 g for 20 min was performed to pellet EVs including ApoBDs (ApoBD enriched samples). It should be noted that no degradative enzymes or additional mechanical force were applied (other than the described procedure such as transferring the apoptotic samples between tubes for differential centrifugation and resuspending cell/vesicle pellets for flow cytometry and immunoblot analysis) to collect the samples.

Preparation of 3K, 16K and 100K samples generated from apoptotic cells

Jurkat T cells were prepared in serum-free RPMI supplemented with 1x Insulin-Transferrin-Selenium (ITS) (Thermo Fisher Scientific). Apoptosis was induced via UV irradiation as described above, followed by incubation at 37°C under a humidified atmosphere with 5% CO_2 for 4 h (control samples were incubated under the same conditions in the absence of UV irradiation). Samples were first centrifuged at 300 g for 10 min and cell pellets were collected. Sequential centrifugation was then performed on cell-free supernatants: Samples were centrifuged at 3,000 g for 20 min. Pellets were then collected ("3k") and supernatants were centrifuged at 16,000 g for 40 min. Pellets were then collected ("16k") and supernatants were centrifuged at 100,000 g followed by collection of pellets ("100k"). All pellets were gently resuspended by pipetting and washed in 1 x PBS followed by a second centrifugation step. Centrifugation at 300 and 3,000 g was performed on an Allegra® X-15R Centrifuge and Eppendorf 5415 R centrifuge (Eppendorf). Centrifugation at 16,000 g was performed on an Optima™ L-100 XP Ultracentrifuge, SW28 (Beckman Coulter) and Eppendorf 5415 R centrifuge. Centrifugation at 100,000 g was performed on an Optima™ L-100 XP Ultracentrifuge and an Optima™ Max-MP Ultracentrifuge, TLA55 (Beckman Coulter). Samples were stored at −80°C until required.

Flow cytometry

The level of apoptosis and ApoBD formation was quantified by flow cytometry as per previous studies [39]. Briefly, samples were incubated in a final concentration of 1× annexin A5 (A5) binding buffer (Thermo Fisher Scientific), 1 in 200 A5-FITC (Thermo Fisher Scientific) and 1 μM TO-PRO-3 (Thermo Fisher Scientific) for 10 min at room temperature in the dark. Samples were then kept on ice and in the dark until flow cytometry analysis using the BD FACSCanto II (FSC resolution of 1 μm, BD Biosciences). Notably, for adherent cells like human LIM1215 colorectal epithelial cells, only apoptotic cells and ApoBDs that are detached from the culture plates during the progression of apoptosis were analysed and no degradative enzymes or additional mechanical force were applied. For size determination of ApoBDs, polystyrene microspheres of 4 μm, 6 μm, 10 μm and 15 μm (Thermo Fisher Scientific) were prepared as per manufacturer's instructions and quantified by flow cytometery alongside ApoBDs. Resultant data were analysed using FlowJo software version 8.8.10 (Tree Star) and electronic gating strategy was applied as described previously [39]. It should be noted that the FACSCanto II flow cytometer used in this study was not calibrated for small particle analysis. Nevertheless, it is possible that large MV-like vesicles were detected and included in the flow cytometery analysis.

Confocal microscopy

Samples in 1% BSA/1× A5 binding buffer/RPMI were stained with A5-FITC or A5-APC and seeded into wells of a Lab-Tek II 8-well chamber slide (Nunc). Live microscopy was performed on either a Zeiss Spinning disk, LSM 780 or LSM 800 confocal microscope (Zeiss) at 37°C in a humidified atmosphere containing 5% CO_2, and using a 63× oil immersion objective. For experiments involving phosphatidylserine (PtdSer) detection on ApoBDs, images were collected over approximately 1 h. For experiments in which non-UV-irradiated cells and ApoBD stability were monitored, time-lapse microscopy was performed over 4 to 6 h. All images were analysed using ZEN Lite 2.3 program (Zeiss).

Immunoblotting

Immunoblotting of cell and ApoBD samples: Cell and ApoBD samples were collected and lysed in lysis buffer (20 mM HEPES pH 7.4, 1%, IGEPAL® CA-630, 10% glycerol, 1% Triton X-100, 150 mM NaCl, 50 mM NaF, protease inhibitor cocktail tablet (Roche)). Next, 20–40

μg of protein was separated on a 12% SDS-PAGE gel and proteins were transferred to a nitrocellulose membrane. Immunoblotting was performed with the following antibodies: PANX1 (Clone D9M1C, Cell Signaling Technology), ROCK1 (Clone C8F7, Cell Signaling Technology), PARP1 (Clone 46D11, Cell Signaling Technology) and β-actin (Clone AC-74, Sigma-Aldrich).

Immunoblotting of EVs isolated via differential centrifugation: Cell pellets were lysed in Cytobuster Protein Extraction Reagent (Merck Millipore) to acquire whole cell lysates (WCL). WCL, 3k, 16k and 100k EV pellets were then treated with LDS loading dye and DTT followed by heating at 90°C for 5 min. 5 μl of protein were then separated on a 12% SDS-PAGE gel. Gels were stained with SYPRO® Ruby Protein Gel Stain (Thermo Fisher Scientific) according to manufacturer's instructions. Protein quantification by densitometry was then performed using ImageJ software. Next, 20–40 μg of protein was separated on a 12% SDS-PAGE gel (omitting DTT and sample heating steps for gels run under non-denaturing conditions) and proteins were transferred to PVDF membranes. Immunoblotting was performed with the following antibodies: Alix (Clone 3A9, Cell Signaling Technology), CD81 (Clone M38, Thermo Fisher Scientific) (under non-denaturing conditions) and BiP/GRP78 (Clone 40/BiP, BD Biosciences).

LDH release assay

The release of LDH by isolated ApoBDs was determined using the LDH Cytotoxicity Assay Kit II (Abcam). Briefly, following apoptosis induction, ApoBDs were isolated via differential centrifugation as per above. Isolated ApoBDs were then incubated at 37°C in a humidified atmosphere with 5% CO_2 for 0, 3 or 6 h. Total lysis was determined by treatment of ApoBDs with LDH kit lysis buffer for 30 sec. All samples were then pelleted by centrifugation at 3,000 g for 5 min, with supernatant collected and analysed as per the manufacturer's instructions. Absorbance readings of LDH reaction products were measured at 450 nm using a SpectraMax M5^e plate reader (Molecular Devices).

Results

Size of ApoBD

The diameter of an EV has been an important criterion to distinguish the major subtypes of EVs including exosomes, microvesicles, ApoBDs and oncosomes [1,2,19,58]. Although the general conception of ApoBDs being 1–5 μm in diameter is a relatively good guideline, it is also clear that this description of ApoBDs needs to be revised. In particular, the size of ApoBDs should be cell type dependent due to differences in cell size and the mechanism of ApoBD formation (Table 1). To this end, we monitored ApoBDs generated from human Jurkat T cells, LIM1215 colon carcinoma cells and THP-1 monocytic cells and found that a subset of ApoBDs derived from these human cell lines was as large as 8–10 μm [39] (Figure 1(a,b)), which are larger than some mouse haematopoietic cells [36,59–61]. Thus, it may not be appropriate to set the upper limit of ApoBDs as 5 μm in diameter for all cell types. Furthermore, ApoBDs derived from human monocytes are generated predominately through the fragmentation of thin "beads-on-a-string" membrane protrusions called beaded apoptopodia [45,62]. We monitored the formation of beaded apoptopodia on apoptotic THP-1 monocytic cells and observed that many of the connecting "beads" of the beaded apoptopodia had a diameter of less than 1 μm (Figure 1(c)), suggesting the fragmentation of these membrane protrusions could generate ApoBDs smaller than 1 μm. Thus, setting the lower limit of ApoBDs as 1 μm in diameter may not be suitable for cells that undergo apoptotic cell disassembly via a beaded apoptopodia-dependent mechanism.

Positive markers of ApoBDs

Defining specific markers that could help distinguish different EV subtypes is a major goal in the field [7,8]. Depending on the nature of these markers (i.e. surface exposed or intracellular), they could be used to detect and isolate EV of interest or validate the EV subtypes present in a sample [7,8]. To date, markers associated with ApoBDs include PtdSer (a phospholipid exposed on the surface of apoptotic cells and ApoBDs to promote recognition and clearance by phagocytes [13]), nuclear proteins and DNA [1–3], as well as calreticulin [28,62], calnexin [63] and BiP/GRP78 [64]. It should be noted that these markers are not necessarily exclusive on/in ApoBDs compared to other EV subtypes [2,28]. In this section, we will evaluate the properties of some of these markers on/in ApoBDs.

Firstly, protein characterization by immunoblotting was performed on Jurkat T cells-derived EVs isolated via 3k, 16k and 100k differential centrifugation in order to compare distribution of typical EV markers in 16k and 100k samples with 3k samples (i.e. samples containing ApoBDs). Endoplasmic reticulum resident

Table 1. Current and proposed criteria to define ApoBDs.

Current Criteria	Proposed	
	Criteria	Rationale / discussion
Detection: Visualization of ApoBDs by light microscopy or electron microscopy [33–38]. Quantification of ApoBDs by flow cytometry [39–42].	• For *in vitro* studies, visualization of ApoBD formation (i.e. morphological steps of apoptotic cell disassembly) by live time-lapse microscopy. • Visualization of ApoBDs by electron microscopy only when appropriate. • Monitor the level of apoptosis. • For both microscopy and flow cytometry approaches to detect ApoBDs, criteria below (size, markers and other properties) should be considered.	• Provides evidence that ApoBDs are indeed generated from cells undergoing apoptosis. • Electron microscopy analysis is suitable to monitor ApoBDs in tissue samples [33,48,55], however, additional sample processing steps may alter ApoBD properties. • Provides evidence that apoptosis did occur as this is the prerequisite for ApoBD formation. • Provides evidence that the vesicles observed are indeed ApoBDs and not other types of extracellular vesicles.
Size: 1–5 μm in diameter [3,19–22,33–38].	• The lower and upper limit of ApoBD diameter should be cell type dependent.	• The size of ApoBDs will vary between cell types, likely due to differences in cell size and the mechanism of ApoBD formation.
Markers: PtdSer exposure [39,53], contains nuclear proteins and DNA [1–3,24,38,81,82], enrichment in calreticulin [28,62].	• ApoBDs can be PtdSerIntermediate or PtdSerLow. • Cell type-specific markers are retained on ApoBDs [57]. • ApoBDs can be with or without DNA/nuclear proteins [45,53]. • For immunoblot analysis of purified ApoBDs, a number of caspase 3/7-cleaved plasma membrane and cytoplasmic proteins should be monitored.	• PtdSer exposure on ApoBDs is a spectrum. • Cell type-specific markers are retained on ApoBDs but at a markedly reduced level compared to apoptotic and viable cells [57]. • Whether DNA and nuclear proteins are distributed into ApoBDs is cell type dependent (likely due to differences in the mechanism of ApoBD formation) and not all ApoBDs contain these nuclear materials [45,53]. • Although caspases could be active under non-apoptotic conditions, monitoring proteins that are cleaved by caspase 3/7 during apoptosis in purified ApoBDs provides additional evidence that the purified sample contain ApoBDs. It should be noted that determining the level of calreticulin will further validate the presence of ApoBDs [28,62].
Other properties: Lysed [67].	• ApoBDs can be both intact and lysed (i.e. membrane permeabilized, leading to leakage of luminal material).	• ApoBDs generated under *in vitro* conditions will become permeabilized over time.

protein BiP/GRP78 was detected in 3k but not 16k or 100k fractions, whereas tetraspanin membrane protein CD81 and ESCRT-associated protein Alix were most abundant in 16k and 100k fractions (Supplementary Figure 2).

The ability of apoptotic cells to expose PtdSer via a caspase-dependent mechanism is a relatively well-described process, in particular through the activation of the scramblase Xkr8 [65] and inhibition of flippases ATP11A and ATP11C [66]. Since the formation of ApoBDs is a somewhat late event during the progression of apoptosis, at a stage that PtdSer is already exposed on the dying cell, it is not surprising that PtdSer can be found on the surface of ApoBDs [36,39]. Despite the fact that PtdSer can also be detected on smaller EVs like [2,67–69], PtdSer is often used as a positive marker for ApoBDs [39]. Notably, when we monitored the exposure of PtdSer on ApoBDs generated from THP-1 and LIM1215 cells treated with UV to induce apoptosis, ApoBDs were found to be either PtdSer[Intermediate] or PtdSer[Low] based on A5 (a PtdSer-binding protein) staining as monitored by confocal microscopy (Figure 2(a,b)), indicating PtdSer exposure alone

may not be a suitable marker to either include or exclude a certain vesicle population to be classified as ApoBDs. It should be noted that it is possible for PtdSer[Low] ApoBD-like vesicles to be released from non-apoptotic cells. To address this, we performed live time-lapse microscopy and did not observe ApoBD-like vesicles being released from viable cells (cells that exhibited no apoptotic morphologies like cell detachment, cell rounding, membrane blebbing and thin membrane protrusion formation) (Supplementary Video 4 and 5).

Proteolytic cleavage of cellular proteins by executioner caspases like caspase 3 and 7 can facilitate the demolition, disassembly and clearance of apoptotic cells [13,19,70]. Thus, it is logical to assume that certain caspase-cleaved proteins can be detected in ApoBDs. To test this, we monitored the expression of well-characterized caspases 3 and 7 substrates (Figure 3(a)) including PANX1 (located at the plasma membrane) [71], ROCK1 (located in the cytosol) [46,72] and PARP1 (located in the nucleus) [73] in ApoBD depleted and ApoBD enriched samples generated from UV-irradiated THP-1 monocytic cells (Figure 3(b),
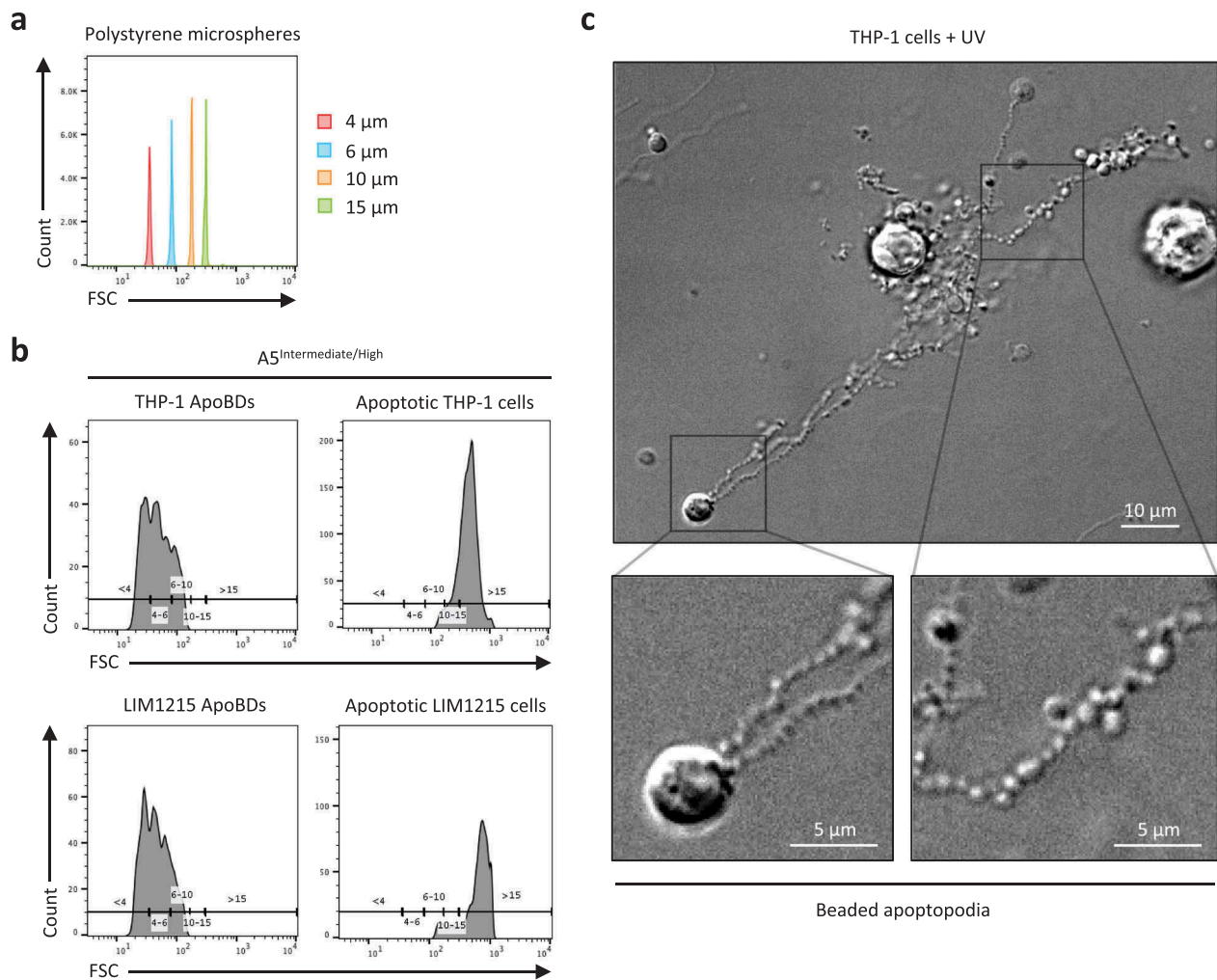
Figure 1. Monitoring the size distribution of ApoBDs. (a) Histogram plots of 4 μm, 6 μm, 10 μm and 15 μm polystyrene microspheres, monitored in forward scatter (FSC) by flow cytometry. (b) A5$^{Intermediate/High}$ apoptotic bodies (ApoBDs) and apoptotic cells generated from THP-1 and LIM1215 cells 4 h post-UV irradiation. Events were distributed into size ranges (μm) of <4, 4–6, 6–10, 10–15 and >15 based on bisector tool analysis of polystyrene microspheres in (a), using FlowJo software. Data are representative of two independent experiments. (**c**) Live differential inference contrast (DIC) microscopy image of a THP-1 cells undergo apoptotic cell disassembly. THP-1 cells were induced to undergo apoptosis by UV irradiation and generate ApoBDs predominately via the fragmentation of beaded apoptopodia. Scale bar, 5 or 10 μm as indicated. Data are representative of at least three independent experiments.

Supplementary Figure 3 for electronic gating strategy for analysis of cells and ApoBDs). It should be noted that the formation of ApoBDs by THP-1 cells occurs via a beaded apoptopodia-dependent mechanism [45] (Figure 1(a)). As expected, caspase-cleaved PANX1 and ROCK1 were readily detected in the ApoBD enriched sample (Figure 3(c,d)). Since nuclear proteins are not distributed into ApoBDs generated from THP-1 cells [45], PARP1 and caspase-cleaved PARP1 were not detected in the ApoBD enriched sample (Figure 3(c)). Although caspases like caspase 3 can be activated in certain non-apoptotic settings [74], monitoring the presence of caspase-cleaved proteins can provide additional evidence to determine whether ApoEVs are present in the sample.

Additional properties of ApoBDs

If an apoptotic cell is not removed by a phagocyte in a timely manner, the cell will progress to secondary necrosis following plasma membrane permeabilization [75]. Loss of plasma membrane integrity can lead to the release of intracellular contents that could promote unwanted inflammation as well as autoimmunity [75]. Thus, whether apoptotic cells and ApoBDs can maintain an intact membrane has significant functional
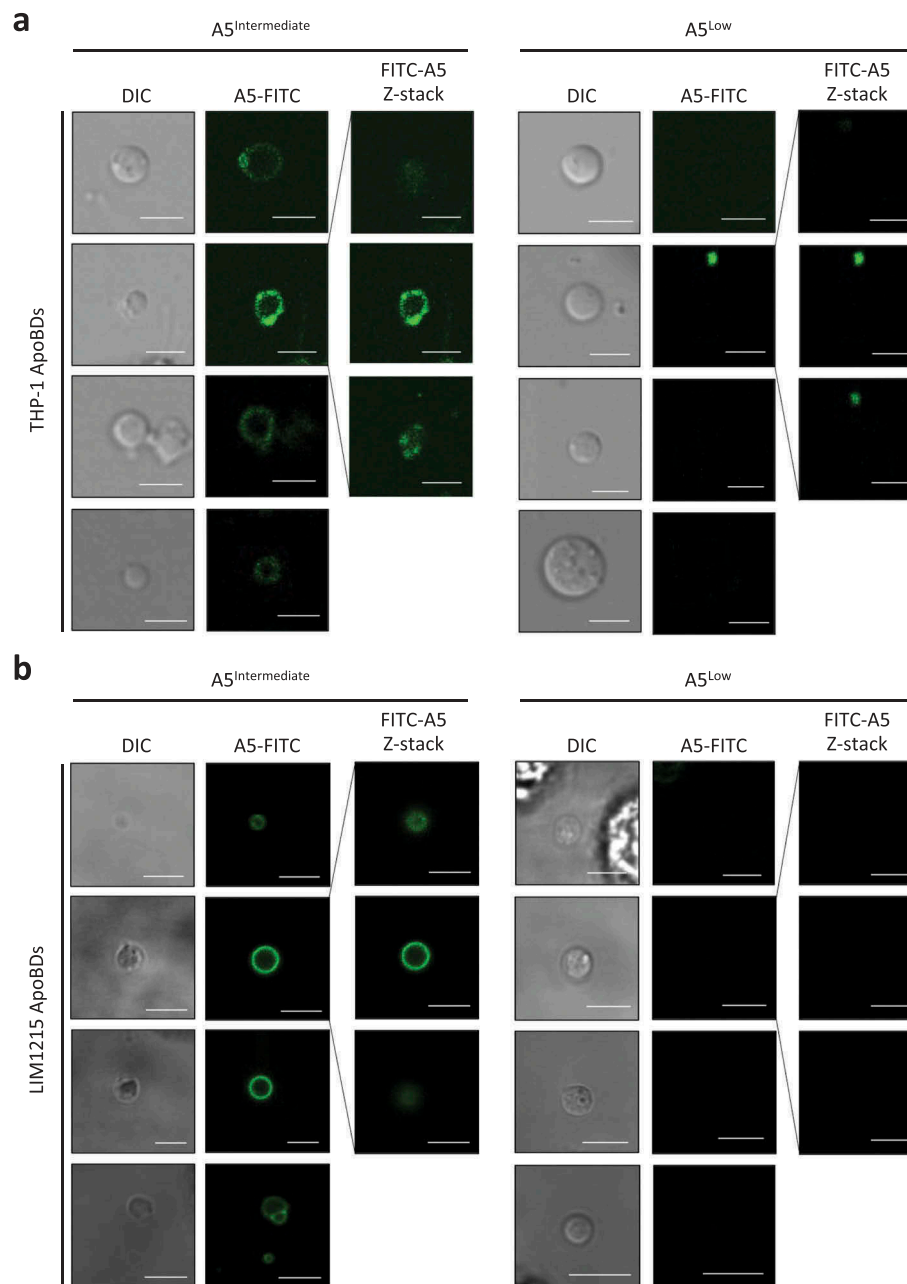
Figure 2. Phosphatidylserine exposure on ApoBDs is a spectrum. A5-FITC staining of phosphatidylserine (PtdSer) on ApoBDs generated from THP-1 (a) and LIM1215 (b) cells, as determined by confocal microscopy. A selection A5^{Intermediate} and A5^{Low} ApoBDs are shown. Selected ApoBDs are displayed as z-stack images to show the distribution of A5-FITC staining on ApoBDs. Scale bar, 5 μm. Data are representative of at least three independent experiments.

implications. Surprisingly, ApoBDs have been described in the field of EVs as lysed vesicles [67] (interpreted as membrane permeabilized vesicles, which can allow transit of luminal material to the extracellular environment). Although a significant proportion of ApoBDs can undergo membrane permeabilization immediately after their formation [40], the progression of ApoBD lysis has not been fully defined. To this end, we have established three experimental approaches to monitor the stability of ApoBDs

(Figure 4(a)). First, ApoBDs generated from human Jurkat T cells and THP-1 monocytic cells were isolated using a recently described differential centrifugation approach [57] and the purity of ApoBDs was confirmed by flow cytometry (Figure 4(b)). ApoBD lysis at a population level was determined based on the release of the cytosolic enzyme lactate dehydrogenase (LDH, ~140 kDa) [76] from isolated ApoBDs. Consistent between ApoBDs derived from Jurkat and THP-1 cells, approximately 40% and 80% of ApoBDs
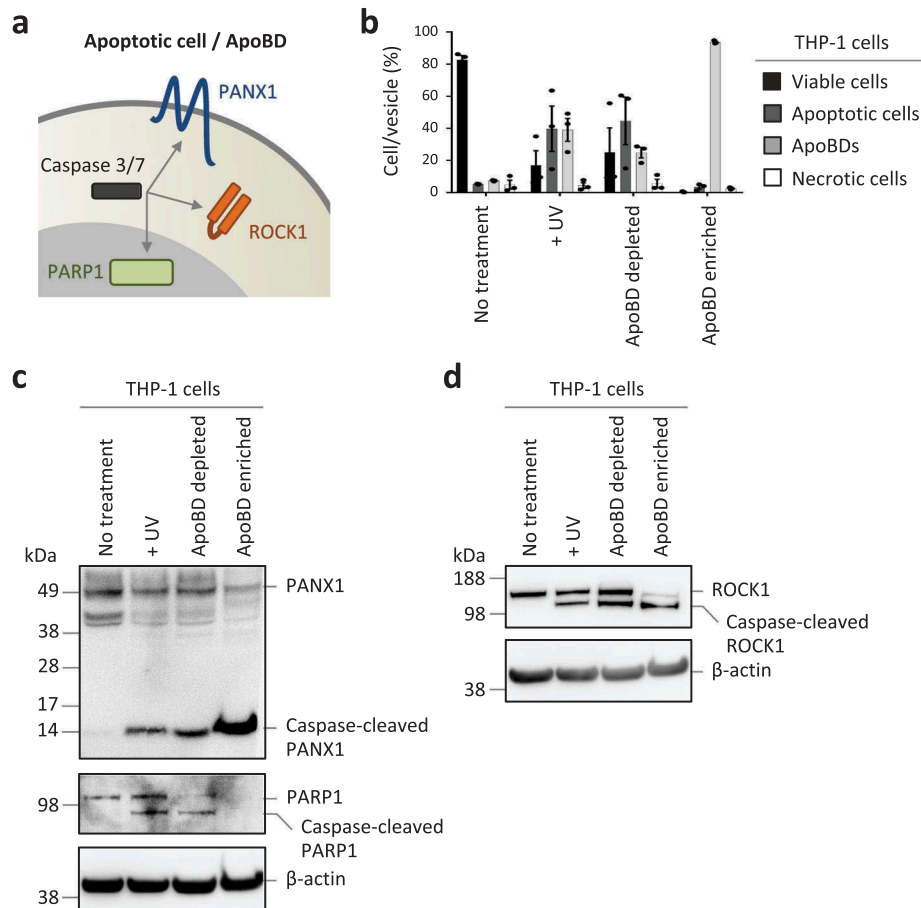
Figure 3. Monitoring caspase-cleaved substrates in purified ApoBDs. (a) Schematic of caspase 3/7 targeting substrates at the plasma membrane, cytoplasm and nucleus. (b) Flow cytometry analysis of the relative levels of viable cells, apoptotic cells, ApoBDs and necrotic cells in untreated, UV-treated, ApoBD depleted and ApoBD enriched samples ($n = 3$). THP-1 monocytes were used as a model cell line. The presence of (c) PANX1 and caspase-cleaved PANX1, PARP1 and caspase-cleaved PARP1, (d) ROCK1 and caspase-cleaved ROCK1 in untreated and apoptotic samples was determined by immunoblotting. Data are representative of at least two independent experiments.

underwent lysis at 3 and 6 h post isolation, respectively (Figure 4(c)). To visualize the membrane permeabilization event at a single ApoBD level, live time-lapse microscopy was performed using the PANX1$^{-/-}$ GFP$^+$ mCherry$^+$ Jurkat T cells induced to undergo apoptosis by UV irradiation and stained with A5-APC to label ApoBDs (Figure 4(d)). Due to the loss of PANX1, a key negative regulator of ApoBD formation [36], these cells can generate a large amount of ApoBDs during apoptosis. Loss of mCherry fluorescence signal in ApoBDs, indicative of mCherry (~29 kDa) release into the culture supernatant, was used as a measure of ApoBD lysis (Figure 4(d,e)). Lastly, utilizing a similar experimental system and previously established flow cytometry-based method to monitor ApoBD formation and contents [39,53], ApoBD lysis was determined by monitoring the level of GFP fluorescence signal in ApoBDs (Figure 4(f), Supplementary Figure 4 for electronic gating strategy for analysis of ApoBD lysis). Similar to

LDH release and time-lapse microscopy-based approaches, ApoBDs progressively lyse over time as determined by flow cytometry (Figure 4(f)). Collectively, these data suggest that ApoBDs are not simply membrane permeabilized vesicles and, approximately 50% of ApoBDs generated from T cells and monocytes could remain intact 3–4 h post isolation/ formation under *in vitro* conditions.

Discussion

Unlike other types of EVs such as exosomes, microvesicles and large oncosomes, ApoBDs are produced only by apoptotic cells that have undergone the apoptotic cell disassembly process. Therefore, it is highly recommended that if ApoBDs are studied and/or isolated under *in vitro* conditions, the levels of apoptosis and/or the cell disassembly process are monitored
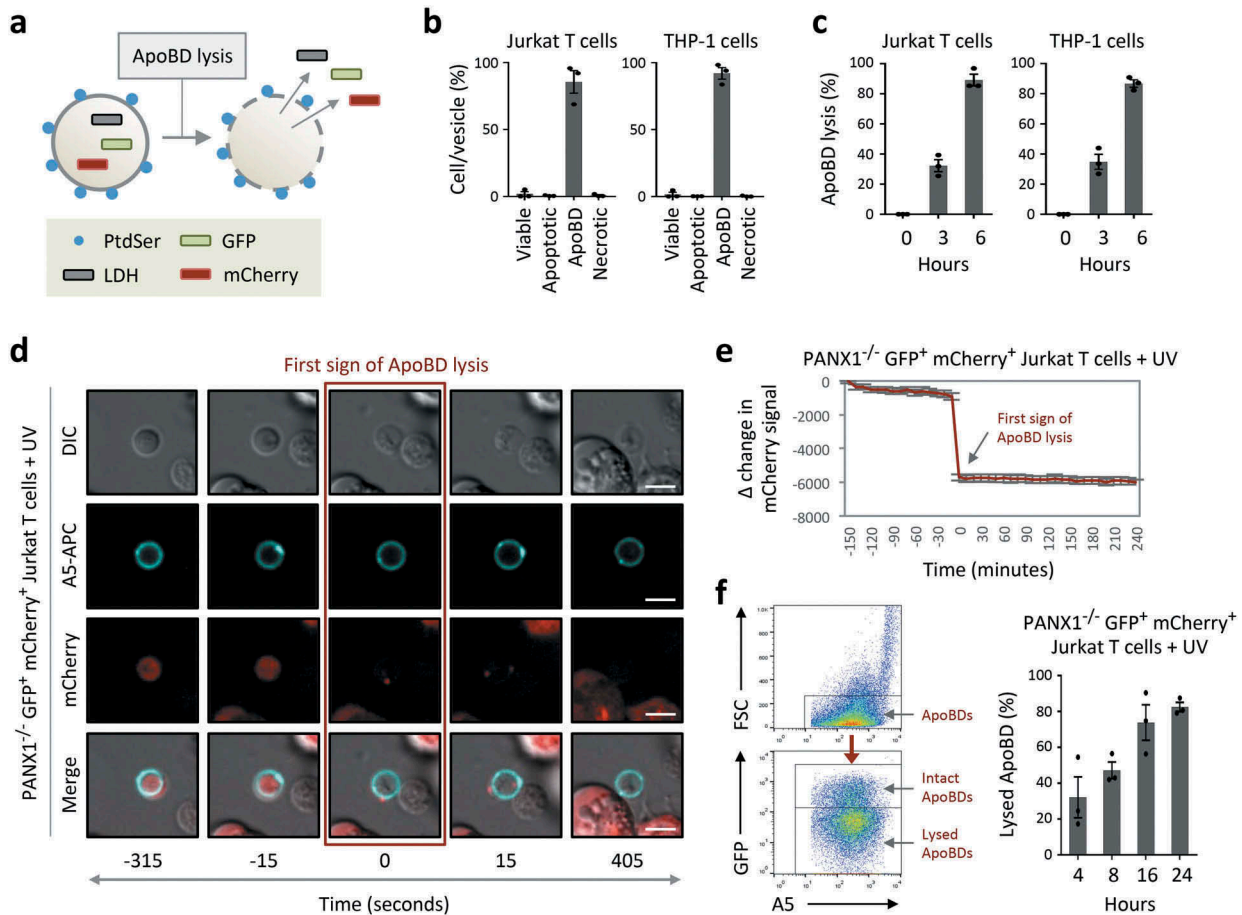
Figure 4. ApoBDs undergo lysis over time. (a) Schematic of the release of intracellular proteins such as lactate dehydrogenase (LDH) and fluorescent proteins GFP and mCherry from ApoBD undergoing membrane lysis. (b) Flow cytometry analysis of ApoBD enriched samples, enriched by differential centrifugation, to determine ApoBD purity ($n = 3$). (c) ApoBD enriched samples were incubated for 0–6 h, and the level of ApoBD lysis determined by LDH release ($n = 3$). (d) Time-lapse images monitoring A5+ ApoBDs generated from PANX1−/− GFP+ mCherry+ Jurkat T cells. Scale bar, 5 μm. Data are representative of at least three independent experiments. (e) Loss of mCherry intensity in individual ApoBDs was quantified from microscopy images using the Zeiss Zen Lite 2.3 software and normalized to first sign of ApoBD lysis ($n = 15$). Units shown are arbitrary and Δ change in mCherry signal was determined by subtracting the mCherry signal at −150 min from the mCherry signal from all time points. (f) Monitoring ApoBD lysis by flow cytometry based on the loss of GFP signal in ApoBDs. Left, flow cytometry plots of electronic gating strategy used for analysing ApoBD lysis. Right, flow cytometry analysis of ApoBD lysis in UV-treated PANX1−/− GFP+ mCherry+ Jurkat T cells. Cells were incubated for 4 to 24 h post UV treatment ($n = 3$). Error bars represent s.e.m.

(Table 1, Figure 5). It should be noted that the presence of larger EVs in a sample (e.g. EVs that are >1 μm in diameter) does not necessarily indicate they are ApoBDs. To support this argument, large oncosomes (>1 to >10 μm in diameter) [77] were found to be distinct from ApoBDs based on the demonstration that apoptosis was not evident in culture conditions where large oncosomes were generated from human DU145 prostate cancer cells [78]. Similarly, we have also demonstrated previously that the plant defensin NaD1 can induce primary necrosis but not apoptosis [39,76,79]. However, Jurkat T cells treated with NaD1 resulted in the formation of EVs that resemble ApoBDs [39]. Thus, if apoptosis was not monitored in complement to EV detection, an incorrect conclusion could

have been made. Nevertheless, it is understandable that if ApoBDs were isolated from/detected in, for example, in vivo or patient samples, it may not be feasible to monitor the level of apoptosis. In these settings, monitoring caspase-cleaved proteins in EV samples as suggested in this study would provide complementary evidence that the sample is likely to contain EVs generated from apoptotic cells. Furthermore, it is worth noting that ApoBDs and large oncosomes are overlapping in size [53,58,78,80], both can be stained positively by propidium iodide (most likely when the vesicles become permeabilized) [40,42,58], and it is currently undetermined whether large oncosomes can expose a sufficient amount of PtdSer for A5 staining. Thus, it could be difficult to distinguish ApoBDs from
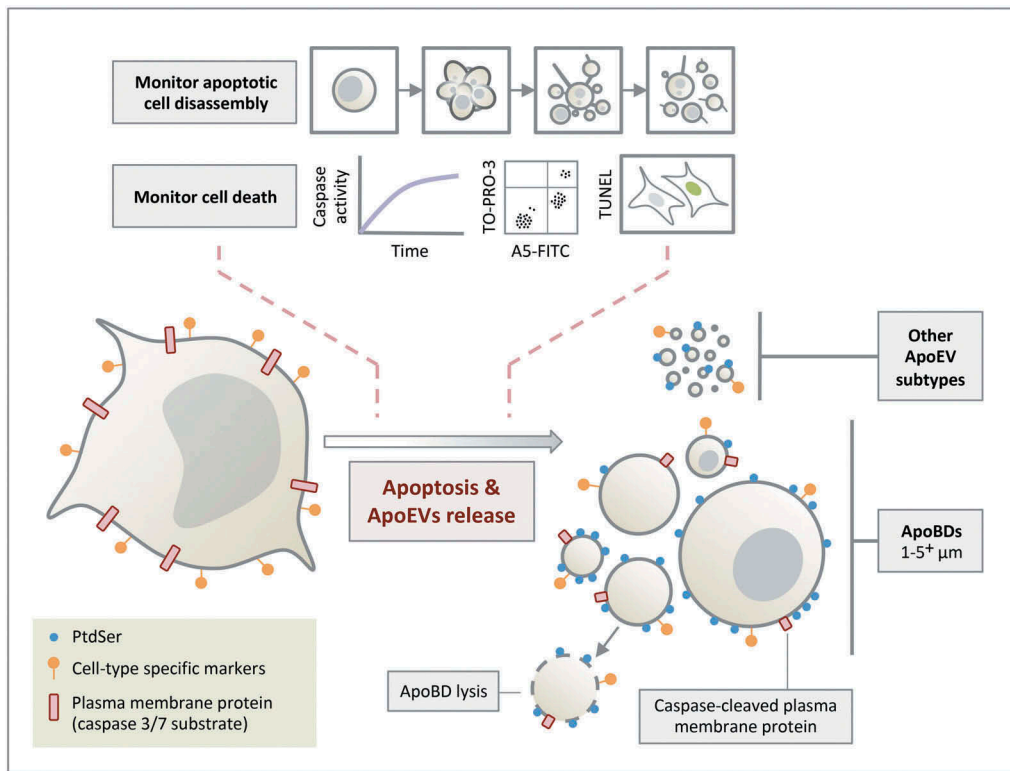
Figure 5. Formation of ApoEVs during apoptosis. ApoBDs and other ApoEV subtypes are generated during apoptosis. Although PtdSer and cell-type specific markers can be found on ApoEVs, these ApoEVs display less PtdSer and cell-type specific marker compared to apoptotic cells. Caspase-cleaved plasma membrane proteins (and cytoplasmic proteins, not depicted in the schematic) can be found in ApoBDs. ApoBDs will undergo membrane lysis (i.e. become secondary necrotic) over time under *in vitro* conditions. The progression of cell death and/or apoptotic cell disassembly should be monitored in ApoEV studies.

large oncosomes, especially if these EV subtypes were isolated from tissue samples. However, since large oncosomes are generated under non-apoptotic conditions [78], large oncosomes are unlikely to contain caspase-cleaved proteins like ApoBDs.

Although certain EV subtypes have overlapping size range [1–6], size is a criterion often used to distinguish different subtypes of EVs. As described above, it is important to acknowledge the possibility that ApoBDs generated from certain cell types could exist outside the traditional range of 1–5 µm, as the size of ApoBDs could be dependent on the size of the cell and the mechanism of apoptotic cell disassembly. Thus, it may be difficult to clearly distinguish larger ApoBDs from apoptotic cell bodies (a term used to describe the remainder of an apoptotic cell that did not undergo further fragmentation) and smaller ApoBDs from other ApoEV subtypes. It should be noted that the study of ApoBDs and other ApoEV subtypes is still in its infancy, and we do not propose to broaden the size range for ApoBDs but to recommend investigators to carefully evaluate in their experimental systems what should be considered as ApoBDs (e.g. based on the combination of parameters/criteria as suggested in Table 1), rather than making the assumption that ApoBDs are strictly 1–5 µm.

Whether further subdividing ApoBDs into large and small ApoBDs could reveal biologically relevant information remains to be defined.

In addition to PtdSer, cell type-specific markers are also retained on the surface of ApoBDs [53,57], again not surprising as ApoBDs appear to acquire a significant portion of the plasma membrane [36,45]. However, it should be noted that the levels of cell type-specific markers on ApoBDs are markedly lower compared to apoptotic and viable cells, and should be monitored with caution [53]. Furthermore, monitoring the presence of caspase-cleaved proteins could be useful to help distinguish ApoBDs from large oncosomes. Identification of caspase-cleaved proteins is simply a complementary approach to indicate the presence of ApoEVs generated from apoptotic cells in the sample. This further highlights the importance to use multiple approaches and lines of evidence to evaluate what ApoEV subtypes are present in the sample, such as using methods that are suitable to identify ApoEVs of interest, determining the size of ApoEVs, and using ApoEV isolation procedure relevant to a specific cell type.

It is well accepted that nuclear proteins and DNA are found in ApoBDs [1–3], and certain nuclear

proteins like histones as well as the presence of DNA can be used as markers to validate the presence of ApoBDs in a sample [24,38,81,82]. Although these markers can be useful to distinguish ApoBDs from other EV subtypes, it is becoming increasingly clear that ApoBDs may not always contain nuclear materials [53]. For example, ApoBDs generated from monocytes via a beaded apoptopodia-dependent mechanism are devoid of nuclear proteins (Figure 3(a–c)) and DNA [45]. Furthermore, based on the live imaging data available under both *in vitro* and *in vivo* conditions [36,45,83] as well as evidence from flow cytometry and electron microscopy-based analysis [33,53,84], cellular contents are not distributed evenly into ApoBDs and it is unlikely that all ApoBDs will contain a comparable amount of nuclear contents. Thus, caution must be taken when using nuclear materials as a marker for ApoBDs.

Small EVs are thought to be relatively stable and could maintain an intact phospholipid bilayer on the surface [85,86], an important property for the transfer intravesicle biomolecules to recipient cells to mediate intercellular communication. Since ApoBDs have also been proposed to mediate the trafficking of microRNAs [82,87], oncogenes [88], cytokines [24], autoantigens [38,89] and pathogen-derived antigens [90], maintaining an intact membrane would be preferable. It should be noted that the stability of ApoBDs is also an important parameter for any downstream omics analysis as biomolecules like RNA, DNA and proteins can be leaked out of lysed ApoBDs. Likewise, lysis of ApoBDs may release damage-associated molecular patterns (known as DAMPs), which could activate certain cell types, hence important for functional studies downstream. Thus, determining whether ApoBDs are intact and the kinetic of lysis as shown in this study is another property of ApoBDs that should be considered in future studies. Although the methods used in this study to monitor ApoBD lysis may not be suitable to determine the percentage of ApoBD that are intact or lysed for all types of samples (e.g. ApoBDs isolated from primary cells or tissues), it is possible to stain ApoBDs with propidium iodide to monitor vesicle lysis [40]. However, caution must be taken with this approach as this method relies on sufficient amount of DNA and/or RNA retained in lysed ApoBDs.

ApoEVs, in particular ApoBDs, are one the first type of EVs being observed in tissue samples [33]. The formation of ApoBDs is not a rare event *in vitro* or *in vivo* [24,33,36,40,45,83], and the highly organized step-wise progression of ApoBD formation can be readily observed live in cultured cells using standard laboratory microscopes [34]. Nevertheless, ApoBDs are arguably the least characterized EV subtype, possibly due to the notion that they are simply "debris" generated from dying cells and cellular contents are distributed into these vesicles randomly. We hope that the discussion and findings in this study have clarified and extended our understanding of ApoBDs, and encourage investigators to use a combination of parameters/criteria for the characterization of ApoBD in future studies.

Author contributions

I.K.H.P., A.A.B., M.A.F.P., L.J., G.K.A., R.T. designed, performed and analysed most of the experiments with help and input from D.C.O., S.F.R., S.C. and J.P.S. In consultation with I.K.H.P. and A.A.B., C.D.G., M.A.F.P., L.J., G.K.A., R.T., D.C.O., S.F.R., S.C., J.P.S., S.P., B.S., A.H., M.D.H., J.D.Y.C. and T.K.P. provided significant intellectual input into establishing criteria for the characterization of ApoEVs. I.K.H.P. and A.A.B. wrote the manuscript with input from co-authors.

Declaration of interest statement

Funding

ORCID

Ivan K. H. Poon ⓘ http://orcid.org/0000-0002-9119-7173

References

[1] Buzas EI, Gyorgy B, Nagy G, et al. Emerging role of extracellular vesicles in inflammatory diseases. Nat Rev Rheumatol. 2014;10:356–364.
[2] Thompson AG, Gray E, Heman-Ackah, SM, et al. Extracellular vesicles in neurodegenerative disease - pathogenesis to biomarkers. Nat Rev Neurol. 2016;12:346–357.
[3] Karpman D, Stahl AL, Arvidsson I. Extracellular vesicles in renal disease. Nat Rev Nephrol. 2017;13:545–562.
[4] Becker A, Thakur BK, Weiss JM, et al. Extracellular vesicles in cancer: cell-to-cell mediators of metastasis. Cancer Cell. 2016;30:836–848.
[5] Schorey JS, Cheng Y, Singh PP, et al. Exosomes and other extracellular vesicles in host-pathogen interactions. EMBO Rep. 2015;16:24–43.

[6] Yuana Y, Sturk A, Nieuwland R. Extracellular vesicles in physiological and pathological conditions. Blood Rev. 2013;27:31–39.

[7] Coumans FAW, Brisson AR, Buzas EI, et al. Methodological guidelines to study extracellular vesicles. Circ Res. 2017;120:1632–1648.

[8] Lotvall J, Hill AF, Hochberg F, et al. Minimal experimental requirements for definition of extracellular vesicles and their functions: a position statement from the international society for extracellular vesicles. J Extracell Vesicles. 2014;3:26913.

[9] Witwer KW, Soekmadji C, Hill AF, et al. Updating the MISEV minimal requirements for extracellular vesicle studies: building bridges to reproducibility. J Extracell Vesicles. 2017;6:1396823.

[10] Sluijter JPG, Davidson SM, Boulanger CM, et al. Extracellular vesicles in diagnostics and therapy of the ischaemic heart: position paper from the working group on cellular biology of the heart of the european society of cardiology. Cardiovasc Res. 2018;114:19–34.

[11] Thery C, Witwer KW, Aikawa E, et al. Minimal information for studies of extracellular vesicles 2018 (MISEV2018): a position statement of the international society for extracellular vesicles and update of the MISEV2014 guidelines. J Extracell Vesicles. 2018;7:1535750.

[12] Elliott MR, Ravichandran KS. The dynamics of apoptotic cell clearance. Dev Cell. 2016;38:147–160.

[13] Nagata S. Apoptosis and clearance of apoptotic cells. Annu Rev Immunol. 2018;36:489–517.

[14] Cummins NW, Badley AD. Mechanisms of HIV-associated lymphocyte apoptosis: 2010. Cell Death Dis. 2010;1:e99.

[15] Roulston A, Marcellus RC, Branton PE. Viruses and apoptosis. Annu Rev Microbiol. 1999;53:577–628.

[16] Stahnke K, Fulda S, Friesen C, et al. Activation of apoptosis pathways in peripheral blood lymphocytes by in vivo chemotherapy. Blood. 2001;98:3066–3073.

[17] Trowell OA. The sensitivity of lymphocytes to ionising radiation. J Pathol Bacteriol. 1952;64:687–704.

[18] Lynch C, Panagopoulou M, Gregory CD. Extracellular Vesicles Arising from Apoptotic Cells in Tumors: roles in Cancer Pathogenesis and Potential Clinical Applications. Front Immunol. 2017;8:1174.

[19] Atkin-Smith GK, Poon IK. Disassembly of the Dying: mechanisms and Functions. Trends Cell Biol. 2017;27:151–162.

[20] Wickman G, Julian L, Olson MF. How apoptotic cells aid in the removal of their own cold dead bodies. Cell Death Differ. 2012;19:735–742.

[21] Gyorgy B, Szabó TG, Pásztói M, et al. Membrane vesicles, current state-of-the-art: emerging role of extracellular vesicles. Cell Mol Life Sci. 2011;68:2667–2688.

[22] Muhsin-Sharafaldine MR, McLellan AD. Tumor-derived apoptotic vesicles: with death they do part. Front Immunol. 2018;9:957.

[23] Pavlyukov MS, Yu H, Bastola S, et al. Apoptotic cell-derived extracellular vesicles promote malignancy of glioblastoma via intercellular transfer of splicing factors. Cancer Cell. 2018;34(119–135):e110.

[24] Berda-Haddad Y, Robert S, Salers P, et al. Sterile inflammation of endothelial cell-derived apoptotic bodies is mediated by interleukin-1alpha. Proc Natl Acad Sci U S A. 2011;108:20684–20689.

[25] Xie Y, Bai Ou, Yuan J., et al. Tumor apoptotic bodies inhibit CTL responses and antitumor immunity via membrane-bound transforming growth factor-beta1 inducing CD8+ T-cell anergy and CD4+ Tr1 cell responses. Cancer Res. 2009;69:7756–7766.

[26] Kalra H, Gilbert TL, Overly CC. Vesiclepedia: a compendium for extracellular vesicles with continuous community annotation. PLoS Biol. 2012;10:e1001450.

[27] Vallabhaneni KC, Hassler M-Y, Abraham A, et al. Mesenchymal stem/stromal cells under stress increase osteosarcoma migration and apoptosis resistance via extracellular vesicle mediated communication. PloS one. 2016;11:e0166027.

[28] Jeppesen DK, Padula MP, Lu JF, et al. Comparative analysis of discrete exosome fractions obtained by differential centrifugation. J Extracell Vesicles. 2014;3:25011.

[29] Lleo A, Zhang W, McDonald WH, et al. Shotgun proteomics: identification of unique protein profiles of apoptotic bodies from biliary epithelial cells. Hepatology. 2014;60:1314–1323.

[30] Szatanek R, Baran J, Siedlar M, et al. Isolation of extracellular vesicles: determining the correct approach (Review). Int J Mol Med. 2015;36:11–17.

[31] Suchorska WM, Lach MS. The role of exosomes in tumor progression and metastasis (Review). Oncol Rep. 2016;35:1237–1244.

[32] Zaborowski MP, Balaj L, Breakefield XO, et al. Extracellular Vesicles: composition, Biological Relevance, and Methods of Study. Bioscience. 2015;65:783–797.

[33] Kerr JF, Wyllie AH, Currie AR. Apoptosis: a basic biological phenomenon with wide-ranging implications in tissue kinetics. Br J Cancer. 1972;26:239–257.

[34] Tixeira R, Caruso S, Paone S, et al. Defining the morphologic features and products of cell disassembly during apoptosis. Apoptosis. 2017;22:475–477.

[35] Crescitelli R, Lässer C, Szabó TG, et al. Distinct RNA profiles in subpopulations of extracellular vesicles: apoptotic bodies, microvesicles and exosomes. J Extracell Vesicles. 2013;2.

[36] Poon IK, Chiu Y-H, Armstrong AJ, et al. Unexpected link between an antibiotic, pannexin channels and apoptosis. Nature. 2014;507:329–334.

[37] Lazaro-Ibanez ESanz-Garcia A, Visakorpi T, et al. Different gDNA content in the subpopulations of prostate cancer extracellular vesicles: apoptotic bodies, microvesicles, and exosomes. Prostate. 2014;74:1379–1390.

[38] Schiller M, Bekeredjian-Ding I, Heyder P, et al. Autoantigens are translocated into small apoptotic bodies during early stages of apoptosis. Cell Death Differ. 2008;15:183–191.

[39] Jiang L, Tixeira R, Caruso S, et al. Monitoring the progression of cell death and disassembly of dying cells by flow cytometry. Nat Protoc. 2016;4:655–663.

[40] Wickman GR, Julian L, Mardilovich K, et al. Blebs produced by actin-myosin contraction during apoptosis release damage-associated molecular pattern proteins before secondary necrosis occurs. Cell Death Differ. 2013;20:1293–1305.

[41] Wlodkowic D, Telford W, Skommer J, et al. Apoptosis and beyond: cytometry in studies of programmed cell death. Methods Cell Biol. 2011;103:55–98.

[42] Hristov M, Erl W, Linder S, et al. Apoptotic bodies from endothelial cells enhance the number and initiate the differentiation of human endothelial progenitor cells in vitro. Blood. 2004;104:2761–2766.

[43] Osteikoetxea X, Sódar B, Németh A, et al. Differential detergent sensitivity of extracellular vesicle subpopulations. Org Biomol Chem. 2015;13:9775–9782.

[44] Nemeth A, Orgovan N, Sódar BW, et al. Antibiotic-induced release of small extracellular vesicles (exosomes) with surface-associated DNA. Sci Rep. 2017;7:8202.

[45] Atkin-Smith GK, Tixeira R, Paone S, et al. A novel mechanism of generating extracellular vesicles during apoptosis via a beads-on-a-string membrane structure. Nat Commun. 2015;6:7439.

[46] Coleman ML, Sahai EA, Yeo M, et al. Membrane blebbing during apoptosis results from caspase-mediated activation of ROCK I. Nat Cell Biol. 2001;3:339–345.

[47] Thery C, Boussac M, Veron P, et al. Proteomic analysis of dendritic cell-derived exosomes: a secreted subcellular compartment distinct from apoptotic vesicles. J Iimmunol. 2001;166:7309–7318.

[48] Elmore S. Apoptosis: a review of programmed cell death. Toxicol Pathol. 2007;35:495–516.

[49] Saraste A, Pulkki K. Morphologic and biochemical hallmarks of apoptosis. Cardiovasc Res. 2000;45:528–537.

[50] Krysko DV, Vanden Berghe T, D'Herde K, et al. Apoptosis and necrosis: detection, discrimination and phagocytosis. Methods. 2008;44:205–221.

[51] Moss DK, Betin VM, Malesinski SD, et al. A novel role for microtubules in apoptotic chromatin dynamics and cellular fragmentation. J Cell Sci. 2006;119:2362–2374.

[52] Rogers C, Fernandes-Alnemri T, Mayes L, et al. Cleavage of DFNA5 by caspase-3 during apoptosis mediates progression to secondary necrotic/pyroptotic cell death. Nat Commun. 2017;8:14128.

[53] Jiang L, Paone S, Caruso S, et al. Determining the contents and cell origins of apoptotic bodies by flow cytometry. Sci Rep. 2017;7:14444.

[54] Turiak L, Misják P, Szabó TG, et al. Proteomic characterization of thymocyte-derived microvesicles and apoptotic bodies in BALB/c mice. J Proteomics. 2011;74:2025–2033.

[55] Godfraind C, Holmes KV, Coutelier JP. Thymus involution induced by mouse hepatitis virus A59 in BALB/c mice. J Virol. 1995;69:6541–6547.

[56] Aubrey BJ, Kelly GL, Kueh AJ, et al. An inducible lentiviral guide RNA platform enables the identification of tumor-essential genes and tumor-promoting mutations in vivo. Cell Rep. 2015;10:1422–1432.

[57] Atkin-Smith GK, Paone S, Zanker DJ, et al. Isolation of cell type-specific apoptotic bodies by fluorescence-activated cell sorting. Sci Rep. 2017;7:39846.

[58] Di Vizio D, Morello M, Dudley AC, et al. Large oncosomes in human prostate cancer tissues and in the circulation of mice with metastatic disease. Am J Pathol. 2012;181:1573–1584.

[59] Monroe JG, Cambier JC. Sorting of B lymphoblasts based upon cell diameter provides cell populations enriched in different stages of cell cycle. J Immunol Methods. 1983;63:45–56.

[60] Salinas FA, Smith LH, Goodman JW. Cell size distribution in the thymus as a function of age. J Cell Physiol. 1972;80:339–345.

[61] Geissmann F, Jung S, Littman DR. Blood monocytes consist of two principal subsets with distinct migratory properties. Immunity. 2003;19:71–82.

[62] Shin S, Han D, Park MC, et al. Separation of extracellular nanovesicles and apoptotic bodies from cancer cell culture broth using tunable microfluidic systems. Sci Rep. 2017;7:9907.

[63] Lunavat TR, Cheng L, Kim D-K, et al. Small RNA deep sequencing discriminates subsets of extracellular vesicles released by melanoma cells–evidence of unique microRNA cargos. RNA Biol. 2015;12:810–823.

[64] Casciola-Rosen LA, Anhalt G, Rosen A. Autoantigens targeted in systemic lupus erythematosus are clustered in two populations of surface structures on apoptotic keratinocytes. J Exp Med. 1994;179:1317–1330.

[65] Suzuki J, Denning DP, Imanishi E, et al. Xk-related protein 8 and CED-8 promote phosphatidylserine exposure in apoptotic cells. Science. 2013;341:403–406.

[66] Segawa K, Kurata S, Yanagihashi Y, et al. Caspase-mediated cleavage of phospholipid flippase for apoptotic phosphatidylserine exposure. Science. 2014;344:1164–1168.

[67] Boulanger CM, Loyer X, Rautou PE, et al. Extracellular vesicles in coronary artery disease. Nat Rev Cardiol. 2017;14:259–272.

[68] Sharma R, Huang X, Brekken RA, et al. Detection of phosphatidylserine-positive exosomes for the diagnosis of early-stage malignancies. Br J Cancer. 2017;117:545–552.

[69] Nakai W, Yoshida T, Diez D, et al. A novel affinity-based method for the isolation of highly purified extracellular vesicles. Sci Rep. 2016;6:33935.

[70] Taylor RC, Cullen SP, Martin SJ. Apoptosis: controlled demolition at the cellular level. Nat Rev Mol Cell Biol. 2008;9:231–241.

[71] Chekeni FB, Elliott MR, Sandilos JK, et al. Pannexin 1 channels mediate 'find-me' signal release and membrane permeability during apoptosis. Nature. 2010;467:863–867.

[72] Sebbagh M, Renvoizé C, Hamelin J, et al. Caspase-3-mediated cleavage of ROCK I induces MLC phosphorylation and apoptotic membrane blebbing. Nat Cell Biol. 2001;3:346–352.

[73] Chaitanya GV, Steven AJ, Babu PP. PARP-1 cleavage fragments: signatures of cell-death proteases in neurodegeneration. Cell Commun Signal. 2010;8:31.

[74] Kuranaga E. Beyond apoptosis: caspase regulatory mechanisms and functions in vivo. Genes Cells. 2012;17:83–97.

[75] Zhang Y, Chen X, Gueydan C, et al. Plasma membrane changes during programmed cell deaths. Cell Res. 2018;28:9–21.

[76] Poon I, Baxter AA, Lay FT, et al. Phosphoinositide-mediated oligomerization of a defensin induces cell lysis. eLife. 2014;3:e01808.

[77] Meehan B, Rak J, Di Vizio D. Oncosomes - large and small: what are they, where they came from? J Extracell Vesicles. 2016;5:33109.

[78] Di Vizio D, Kim J, Hager MH, et al. Oncosome formation in prostate cancer: association with a region of frequent chromosomal deletion in metastatic disease. Cancer Res. 2009;69:5601–5609.

[79] Baxter AA, Poon IK, Hulett MD. The plant defensin NaD1 induces tumor cell death via a non-apoptotic, membranolytic process. Cell Death Discov. 2017;3:16102.

[80] Johnson SM, Dempsey C, Parker C, et al. Acute lymphoblastic leukaemia cells produce large extracellular vesicles containing organelles and an active cytoskeleton. J Extracell Vesicles. 2017;6:1294339.

[81] Hauser P, Wang S, Didenko VV. Apoptotic Bodies: selective Detection in Extracellular Vesicles. Methods Mol Biol. 2017;1554:193–200.

[82] Zhu Z, Zhang D, Lee, H, et al. Macrophage-derived apoptotic bodies promote the proliferation of the recipient cells via shuttling microRNA-221/222. J Leukoc Biol. 2017;101:1349–1359.

[83] Mayer CT, Gazumyan A, Kara EE, et al. The microanatomic segregation of selection by apoptosis in the germinal center. Science. 2017;358.

[84] Croft DR, Coleman ML, Li S, et al. Actin-myosin-based contraction is responsible for apoptotic nuclear disintegration. J Cell Biol. 2005;168:245–255.

[85] Kumeda N, Ogawa Y, Akimoto Y, et al. Characterization of membrane integrity and morphological stability of human salivary exosomes. Biol Pharm Bull. 2017;40:1183–1191.

[86] Kalra H., Adda CG, Liem M, et al. Comparative proteomics evaluation of plasma exosome isolation techniques and assessment of the stability of exosomes in normal human blood plasma. Proteomics. 2013;13:3354–3364.

[87] Zernecke A, Bidzhekov K, Noels H, et al. Delivery of microRNA-126 by apoptotic bodies induces CXCL12-dependent vascular protection. Sci Signal. 2009;2:ra81.

[88] Bergsmedh A, Szeles A, Henriksson M, et al. Horizontal transfer of oncogenes by uptake of apoptotic bodies. Proc Natl Acad Sci U S A. 2001;98:6407–6411.

[89] Cocca BA, Cline AM, Radic MZ. Blebs and apoptotic bodies are B cell autoantigens. J Iimmunol. 2002;169:159–166.

[90] Winau F, Kaufmann SH, Schaible UE. Apoptosis paves the detour path for CD8 T cell activation against intracellular bacteria. Cell Microbiol. 2004;6:599–607.